Chinese Chemical Letters 35 (2024) 108819

Contents lists available at ScienceDirect

Chinese Chemical Letters

journal homepage: www.elsevier.com/locate/cclet

An AIPE-active fluorinated cationic Pt(II) complex for efficient detection of picric acid in aqueous media

Yingying Yan[1], Wanhe Jia[1], Rui Cai, Chun Liu*

State Key Laboratory of Fine Chemicals, Frontier Science Center for Smart Materials, School of Chemical Engineering, Dalian University of Technology, Dalian 116024, China

ARTICLE INFO

Article history:
Received 30 May 2023
Revised 13 July 2023
Accepted 14 July 2023
Available online 17 July 2023

Keywords:
Pt(II) complexes
Fluorine atom
AIPE activity
Picric acid
Photo-induced electron transfer

ABSTRACT

A novel cationic Pt(II) complex **2** with 2-(2,4-difluorophenyl)pyridine as the cyclometalating ligand and 1,10-phenanthroline as the auxiliary ligand has been synthesized and fully characterized. This complex exhibits much higher aggregation-induced phosphorescent emission activity than that of a non-fluorinated complex **1** in CH_3CN/H_2O. The complex **2** demonstrates efficient detection on picric acid (PA) in CH_3CN/H_2O, providing a high quenching constant ($K_{SV} = 2.3 \times 10^4$ L/mol) and a low limit of detection (LOD = 0.26 μmol/L). In addition, complex **2** shows high selectivity for detection of PA in real water samples. Density functional theory calculations and proton nuclear magnetic resonance spectra suggest that the detection mechanism is attributed to the photo-induced electron transfer.

Aggregation-induced emission (AIE), as an extraordinary photophysical phenomenon, has been recognized as a frontier research topic over the last two decades [1–3]. Soon after the concept of AIE was stated, the AIE-active Re(I) complexes were reported by Manimaran *et al.*, named as aggregation induced phosphorescent emission (AIPE) [4]. In 2008, Zhu *et al.* reported a class of AIPE-active dicationic terpyridyl-platinum(II) complexes [5]. To date, AIPE-active cationic Pt(II) complexes have focused on two-ligand molecular frameworks consisting of one tridentate ligand and one monodentate ligand, while the C^N bidentate ligands modified cationic Pt(II) complexes are still infrequent and need further exploration (Table S1 in Supporting information) [6–10].

As a unique C^N bidentate ligand, 2-(2,4-difluorophenyl)-pyridine (dfppy) can serve as an excellent cyclometalating ligand for tuning the performances of the corresponding cyclometalated Pt(II) complexes [11–14]. Compared to 2-phenylpyridine (ppy), the complexes constructed by dfppy demonstrated impressive photophysical properties [15–18]. Besides, the intermolecular hydrogen bonds induced by fluorine atoms can significantly enhance the molecular aggregation to influence their properties [19]. In 2021, Shahsavari and colleagues reported several dfppy-based Pt(II) complexes, exhibiting higher quantum yields compared to their ppy analogues [13]. Recently, Hamidizadeh *et al.* showed that the emission intensity of the Pt(II) complexes significantly enhanced after replacing ppy with dfppy [14].

Picric acid (PA) is commonly used to manufacture high explosives, posing a serious threat to human life [20]. Hence, it is necessary to develop a sensitive and selective detection method for PA. To date, a number of fluorescent and phosphorescent materials have been synthesized to serve as sensors for PA [21–27]. Among them, Pt(II) complexes are predominantly concentrated on the metallacycles and metallacages from the self-assembly of organoplatinum compounds (Table S2 in Supporting information) [28,29].

Our group has a long-term interest in the relationship between the molecular structures of the cyclometalated Pt(II) and Ir(III) complexes and their properties [30–37]. Recently, we designed and synthesized several AIPE-active cationic Ir(III) complexes, which demonstrated efficient detection of PA in aqueous media [36,37]. However, the development of cyclometalated Pt(II) complexes is far behind in comparison [38]. Specifically, AIPE-active cationic cyclometalated Pt(II) complexes for detecting PA in aqueous media have not been reported. In this study, a novel cationic cyclometalated Pt(II) complex **2** using dfppy as the cyclometalating ligand and 1,10-phenanthroline as the auxiliary ligand has been prepared. The properties of **2** have been systematically investigated compared with a non-fluorinated complex **1**. In addition, the detection of PA using the Pt(II) complex as a probe in aqueous media was studied. The structures of **1** and **2** are depicted in Fig. 1a.

The normalized emission spectra of **1** and **2** in CH_3CN and in the solid state are shown in Fig. 1b. **1** and **2** exhibit evident fine

* Corresponding author.
E-mail address: cliu@dlut.edu.cn (C. Liu).
[1] These authors contributed equally to this work.

https://doi.org/10.1016/j.cclet.2023.108819
1001-8417/

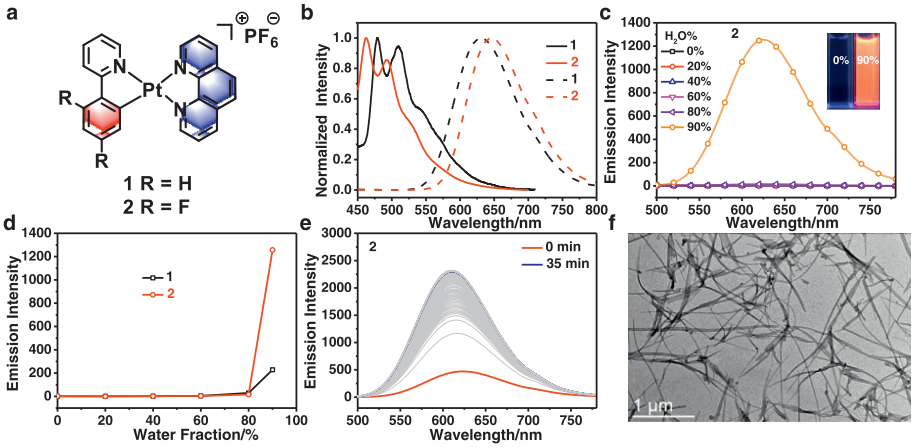

Fig. 1. (a) The structures of **1** and **2**. (b) Normalized emission spectra (solution: solid trace, solid: dash trace) of **1** (black) and **2** (red) at room temperature (50 μmol/L in CH_3CN). (c) Emission spectra of **2** and (d) emission intensity curves of **1** and **2** at 50 μmol/L in CH_3CN/H_2O with different water fractions. (e) Time-dependent emission spectra of **2** (CH_3CN/H_2O, v/v = 1:9, 50 μmol/L). (f) TEM image of aggregates of **2** (CH_3CN/H_2O, v/v = 1:9, 50 μmol/L). The excitation wavelength was 400 nm.

vibronic splitting characteristics at 462–479 nm in CH_3CN, which are assigned to ligand-centered character (^{3}LC) [32]. Introducing fluorine atoms into the benzene ring results in an obvious blue-shift of 17 nm for **2** compared to **1**. This may be due to the fact that fluorine atoms effectively stabilize the highest occupied molecular orbital (HOMO) [13], which can be further supported by theoretical calculations. The complexes exhibit extremely broad, featureless peaks in the solid state, which are considerably different from those in solution. Furthermore, the emission spectra of **1** and **2** in the solid state demonstrate significant red-shift compared to the spectra recorded in CH_3CN, which can be attributed to the emission of the aggregates [39]. In the solid state, the maximum emission wavelengths of **1** and **2** are determined as 631 and 646 nm, and the absolute quantum yields are 38.5% and 34.5%, respectively (Table S3 in Supporting information). The ultraviolet–visible (UV–vis) absorption spectra of **1** and **2** in CH_3CN at room temperature were presented in Fig. S1 (Supporting information) and the detailed photophysical data were listed in Table S3.

The strong emission of complexes in the solid state suggests they are likely to exhibit AIPE activities [40]. To confirm the hypothesis, the emission spectra of the complexes were conducted with different water fractions in CH_3CN/H_2O. As depicted in Fig. 1c and Fig. S2 (Supporting information), **1** and **2** exhibit very weak emission at the water fractions ranging from 0% to 80%, and the emission intensities reach the maximum at a water fraction of 90%, demonstrating obvious AIPE activities. Further analysis reveals that the emission intensity of **2** at the water fraction of 90% is much higher than that of **1** at the same conditions (Fig. 1d), showing that the introduction of fluorine atoms clearly influences the AIPE activity of the complex. This can be assigned to the abundant intermolecular hydrogen bonds induced by the fluorine atoms, which leads to enhanced intermolecular interaction, thus limiting molecular motion and resulting in higher AIPE activity of complex **2** [19].

In this study, we found that the emission intensities of the complexes increased over time at the water fraction of 90% in CH_3CN/H_2O. Thus, we explored the time-dependent emission spectra of **1** and **2**. Fig. 1e and Fig. S3 (Supporting information) show that emission intensities of **1** and **2** are very weak at first, but enhance gradually over time. The relative emission intensity ratios of I_{608}/I_{624} indicate that **2** reaches equilibrium at about 35 min (Fig. S4 in Supporting information). However, the equilibrium time of **1** is obviously shortened, within around 5 min. The results suggest that the presence of fluorine atoms affects the aggregation process of the complex. Furthermore, transmission electron microscopy (TEM) images show that the aggregates of **1** and **2** are nanofibers (Fig. 1f and Fig. S5 in Supporting information).

The UV–vis absorption spectra of **1** and **2** were recorded in CH_3CN/H_2O with different water fractions (Fig. S6 in Supporting information). As the water fraction increases, the absorption peaks below 400 nm decrease gradually and a new absorption tail appears at 450–550 nm. This tail can be assigned to metal-metal-to-ligand charge transfer [7,41].

The electrochemical properties of **1** and **2** in *N,N*-dimethylformamide (DMF) solution were studied by cyclic voltammetry (Fig. S7 in Supporting information). Compared to **1**, the oxidation and reduction potentials of **2** are notably increased. The energy gaps between HOMOs and lowest unoccupied molecular orbital (LUMO) levels of **1** and **2** are 2.16 and 2.24 eV, respectively, which is consistent with the observed blue-shift in the emission spectra (Table S4 in Supporting information) [13,14].

Density function theory (DFT) calculations were used to explore the electronic structures of **1** and **2**. The HOMOs of **1** and **2** are primarily derived from cyclometalating ligands and Pt center, while the LUMOs are mainly distributed on auxiliary ligands and Pt center. The calculated energy gaps for **1** and **2** are 3.53 and 3.68 eV, respectively (Fig. S8 in Supporting information). The introduction of fluorine atoms onto the cyclometalating ligand significantly affected the HOMO level of the complex, leading to a substantial increase in the energy gap.

Inspired by the high AIPE activity of **2**, we used this complex as a probe to detect picric acid (PA) in CH_3CN/H_2O (v/v = 1:9). Complex **2** exhibits strong emission in the absence of PA, but its emission is quenched gradually upon increasing PA concentrations (Fig. 2a). When the concentration of PA reaches 400 μmol/L, 96% of the emission is quenched. The Stern-Volmer plot of I_0/I (I_0 and I represent the emission intensities before and after the addition of PA) *vs.* PA concentrations shows a non-linear relationship in the range of 0–800 μmol/L (Fig. 2b), indicating the presence of both static and dynamic quenching processes [42,43]. The Stern-Volmer plot shows good linearity in the concentrations of PA ranging from 0 to 20 μmol/L (–, inset), which is mainly due to the static quenching [44,45]. The quenching constant is 2.3×10^4 L/mol and the limit of detection (LOD) of **2** is calculated to be 0.26 μmol/L (Figs. S9 and S10 and Table S5 in Supporting information). These results exhibit that complex **2** can be used as a probe for efficient detection of PA in aqueous media.

Considering the sensitive detection of **2** for PA, selective experiments were further conducted. The analytes (nitrobenzene (NB), 1,3-dinitrobenzene (1,3-DNB), nitromethane (NM), phenol, *p*-cresol,

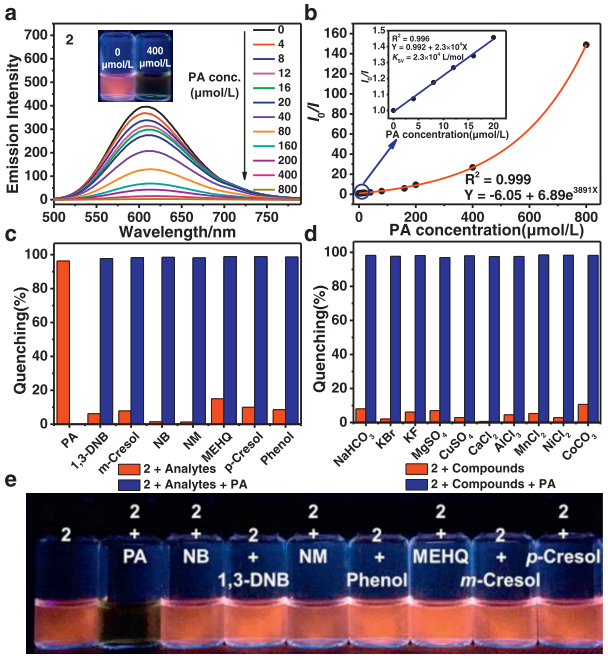

Fig. 2. (a) The emission spectra of **2** at 20 μmol/L in CH_3CN/H_2O (v/v = 1:9) with different concentrations of PA. (b) The Stern-Volmer plot of I_0/I *vs.* the concentration of PA. Insert: the linear part of Stern-Volmer plot in the concentrations of PA ranging from 0 to 20 μmol/L. I_0 represents emission intensity of **2** and I represents emission intensity of **2** containing different amounts of PA. (c, d) Quenching percentages of **2** with different analytes (c) and ionic compounds (d) in CH_3CN/H_2O (v/v = 1:9) before (red) and after (blue) the addition of PA. (e) The photo of the suspensions of **2** upon the addition of various analytes under UV light. The excitation wavelength was 400 nm.

4-methoxyphenol (MEHQ) and *m*-cresol), and the compounds with different ions ($NaHCO_3$, KBr, KF, $MgSO_4$, $CuSO_4$, $CaCl_2$, $AlCl_3$, $MnCl_2$, $NiCl_2$ and $CoCO_3$) were selected to investigate the selectivity for detecting PA. As shown in Fig. S11 (Supporting information), compared with the addition of PA, the emission intensities of **2** do not display a noteworthy alteration upon the addition of other analytes and ionic compounds. The phenomena are also confirmed from the corresponding photos under UV light (Fig. 2e and Fig. S12 in Supporting information) [46]. The above results provide evidence for the high selectivity of complex **2** towards PA. This selectivity may be attributed to the fact that PA acts as a typical electron acceptor, while **2** acts as an excellent electron donor, facilitating a photo-induced electron transfer (PET) process [37,47]. Additionally, the strong electrostatic interactions between PA and **2** can also contribute to the high selectivity [24].

To evaluate the anti-interference ability of a probe, the competitive experiments were studied. The results display that the quenching percentages of **2** caused by PA remain almost constant in the presence of other competitive analytes and ionic compounds (Figs. 2c and d), indicating that **2** exhibits impressive anti-interference ability in the process of PA recognition.

To explore practical applications, **2** was used to detect PA in various natural water samples, including tap water, river water and rainwater. Fig. 3 displays the emission spectra and quenching percentages of **2** in different water samples, suggesting that **2** works effectively for detecting PA in natural water samples (CH_3CN/H_2O, v/v = 1:9). So far, the majority of reported Pt(II) complexes for the detection of PA have been focused on metallacycles and metallacages from the self-assembly of organoplatinum compounds in organic solvents. To the best of our knowledge, this is the first report of the AIPE-active cationic cyclometalated Pt(II) complex for efficient detection of PA in aqueous media. The Pt(II) complex **2** contains a C^N type cyclometalating ligand

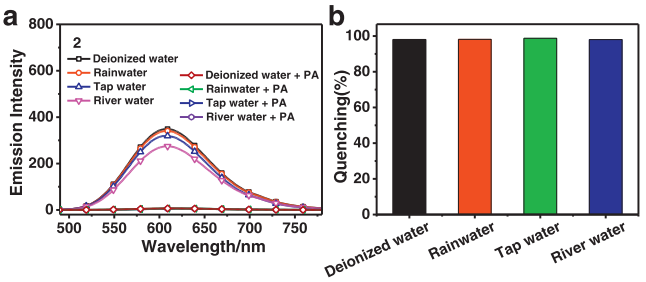

Fig. 3. The emission spectra (a) and quenching percentages (b) of **2** towards PA in different water samples (CH_3CN/H_2O, v/v = 1:9). The excitation wavelength was 400 nm.

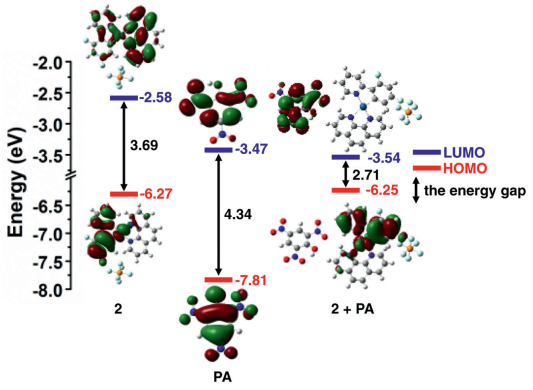

Fig. 4. Calculated energy level diagram of **2**, PA and adduct (**2** + PA).

of 2-(2,4-difluorophenyl)-pyridine and 1,10-phenanthroline as the auxiliary ligand. This complex demonstrates a limit of detection of 0.26 μmol/L and excellent selectivity towards PA in aqueous media. Moreover, it performs well for the detection of PA in natural water samples, providing a practical method for detecting PA.

The emission quenching mechanism of **2** for PA was explored through DFT calculations. Fig. 4 indicates that the LUMO energy of PA (−3.47 eV) is much lower than that of **2** (−2.58 eV), suggesting that a photo-induced electron transfer (PET) process may occur, leading to the emission quenching [48]. Besides, the energy gaps of **2**, PA, and the adduct (**2** + PA) are 3.69, 4.34 and 2.71 eV, respectively. Among them, the energy gap of the adduct (**2** + PA) is the lowest, showing that the adduct is the most stable. In addition, the ^{1}H nuclear magnetic resonance (^{1}H NMR) spectrum of **2** in the presence of PA shows the chemical shifts of proton signals of **2** move towards the high field, supporting the presence of strong electrostatic interactions between PA and **2** (Fig. S13 in Supporting information) [22,49]. These results reveal that the phosphorescent quenching of **2** for the detection of PA is mainly attributed to PET.

In summary, two structurally simple cationic Pt(II) complexes with AIPE activities have been studied. Complex **2** with a dfppy ligand exhibits much higher AIPE activity than a non-fluorinated complex **1**. Complex **2** demonstrates efficient detection on PA with a high quenching constant of 2.3×10^4 L/mol and a low LOD of 0.26 μmol/L in aqueous media. Furthermore, as a sensor for detecting PA, **2** works well in the natural water samples. The detection mechanism is attributed to the photo-induced electron transfer. These findings provide valuable insights in designing efficient AIPE-active Pt(II) complexes for the detection of PA in aqueous media.

Declaration of competing interest

The authors declare that they have no known competing financial interests or personal relationships that could have appeared to influence the work reported in this paper.

Acknowledgments

The authors thank the financial support from the National Natural Science Foundation of China (No. 21978042) and the Fundamental Research Funds for the Central Universities (No. DUT22LAB610).

Supplementary materials

Supplementary material associated with this article can be found, in the online version, at doi:10.1016/j.cclet.2023.108819.

References

[1] J. Luo, Z. Xie, J.W.Y. Lam, et al., Chem. Commun. 18 (2001) 1740–1741.
[2] J. Mei, N.L.C. Leung, R.T.K. Kwok, J.W.Y. Lam, B.Z. Tang, Chem. Rev. 115 (2015) 11718–11940.
[3] X. Li, M. Li, M. Yang, et al., Coord. Chem. Rev. 418 (2020) 213358.
[4] B. Manimaran, P. Thanasekaran, T. Rajendran, et al., Inorg. Chem. 41 (2002) 5323–5325.
[5] M.X. Zhu, W. Lu, N. Zhu, C.M. Che, Chem. Eur. J. 14 (2008) 9736–9746.
[6] J.L.L. Tsai, T. Zou, J. Liu, et al., Chem. Sci. 6 (2015) 3823–3830.
[7] H.K. Cheng, M.C.L. Yeung, V.W.W. Yam, ACS Appl. Mater. Interfaces 9 (2017) 36220–36228.
[8] J. Wu, Y. Li, C. Tan, et al., Chem. Commun. 54 (2018) 11144–11147.
[9] R. Liang, W. Xiong, X. Bai, L. Du, D.L. Phillips, J. Phys. Chem. C 125 (2021) 11432–11439.
[10] X. Yao, W. Zhang, B. Fang, et al., Dyes Pigm. 184 (2021) 108788.
[11] C. Li, L. Xu, J. Li, et al., Dyes Pigm. 209 (2023) 110912.
[12] C.H. Chen, F.L. Wu, Y.Y. Tsai, C.H. Cheng, Adv. Funct. Mater. 21 (2011) 3150–3158.
[13] H.R. Shahsavari, S. Paziresh, New J. Chem. 45 (2021) 22732–22740.
[14] P. Hamidizadeh, R.B. Aghakhanpour, S. Chamyani, et al., Organometallics 41 (2022) 1325–1333.
[15] L. Niu, G. Ren, T. Hou, X. Shen, D. Zhu, Inorg. Chem. Commun. 130 (2021) 108737.
[16] M. Martínez-Junquera, E. Lalinde, M.T. Moreno, et al., Dalton Trans. 50 (2021) 4539–4554.
[17] M. Martínez-Junquera, R. Lara, E. Lalinde, M.T. Moreno, J. Mater. Chem. C 8 (2020) 7221–7233.
[18] L. Schneider, V. Sivchik, K.Y. Chung, et al., Inorg. Chem. 56 (2017) 4459–4467.
[19] X. Yang, H. Guo, X. Xu, et al., Adv. Sci. 6 (2019) 1801930.
[20] X. Liu, Y. Han, Y. Shu, J. Wang, H. Qiu, J. Hazard. Mater. 425 (2022) 127987.
[21] L. Wang, W. Chen, W. Song, et al., Chin. Chem. Lett. 34 (2023) 107291.
[22] S.K. Patra, B. Sen, M. Rabha, S. Khatua, New J. Chem. 46 (2022) 169–177.
[23] F. Zhu, H. Fang, W. Liu, et al., Mater. Lett. 306 (2022) 130957.
[24] S. Jiang, L. Meng, W. Ma, et al., Chin. Chem. Lett. 32 (2021) 1037–1040.
[25] J. Liu, Y. Xu, C. Qin, et al., Dalton Trans. 48 (2019) 13305–13314.
[26] R. Zhang, L. Zhu, B. Yue, Chin. Chem. Lett. 34 (2023) 108009.
[27] N. Yan, J. Song, F. Wang, et al., Chin. Chem. Lett. 30 (2019) 1984–1988.
[28] Y. Hou, S. Li, Z. Zhang, L. Chen, M. Zhang, Polym. Chem. 11 (2020) 254–258.
[29] Y. Hou, R. Shi, H. Yuan, M. Zhang, Chin. Chem. Lett. 34 (2023) 107688.
[30] Y. Yan, Z. Yu, C. Liu, X. Jin, Dyes Pigm. 173 (2020) 107949.
[31] Y. Xing, L. Wang, C. Liu, X. Jin, Sens. Actuators B: Chem. 304 (2020) 127378.
[32] Y. Yan, Z. Yu, J. Wang, C. Liu, Tetrahedron Lett. 119 (2023) 154427.
[33] Y. Chen, Z. Gao, L. Wang, et al., ACS Appl. Polym. Mater. 4 (2022) 1055–1064.
[34] Y. Chen, L. Zhang, L. Wang, L. Guo, C. Liu, Mater. Chem. Front. 21 (2021) 7808–7816.
[35] Y. Chen, Y. Shi, Z. Gao, et al., Angew. Chem. Int. Ed. 62 (2023) e202302581.
[36] P. He, Y. Chen, X. Li, Y. Yan, C. Liu, Chemosensors 11 (2023) 177.
[37] P. He, Y. Chen, X. Li, Y. Yan, C. Liu, Dalton Trans. 52 (2023) 128–135.
[38] P. Maity, A. Bhatt, B. Agrawal, A. Jana, Langmuir 33 (2017) 4291–4300.
[39] Z. Gong, K. Tang, Y. Zhong, Inorg. Chem. 60 (2021) 6607–6615.
[40] L. Wang, Z. Gao, C. Liu, X. Jin, Mater. Chem. Front. 3 (2019) 1593–1600.
[41] B. Li, Z. Liang, H. Yan, Y. Li, Mol. Syst. Des. Eng. 5 (2020) 1578–1605.
[42] Z. Li, Z. Yao, R. Feng, et al., Chin. Chem. Lett. 32 (2021) 3095–3098.
[43] P. Ju, E. Zhang, L. Jiang, et al., RSC Adv. 8 (2018) 21671–21678.
[44] Z. Luo, B. Liu, S. Si, et al., Dyes Pigm. 143 (2017) 463–469.
[45] N. Wang, J. Yang, L. Chen, et al., New J. Chem. 41 (2017) 2786–2792.
[46] L. Zhang, Y. Sun, Y. Jiang, et al., Chin. Chem. Lett. 31 (2020) 2428–2432.
[47] T. Feng, X. Li, J. Wu, C. He, C. Duan, Chin. Chem. Lett. 31 (2020) 95–98.
[48] F. Zu, F. Yan, Z. Bai, et al., Microchim. Acta 184 (2017) 1899–1914.
[49] H. Ma, C. He, X. Li, et al., Sens. Actuators B: Chem. 230 (2016) 746–752.